6-hour interval between the last calibration and the image data collection. The drift was due to flexure from temperature effects and other mechanical stresses, as well as inaccuracies in repositioning the wave front sensor between the focal positions for the natural guide star and the laser star. These errors can be reduced by calibrating more frequently.

NOTES AND REFERENCES

1. H. W. Babcock, *Publ. Astron. Soc. Pac.* **65**, 229 (1953); *Science* **249**, 253 (1990).
2. L. A. Thompson, *Phys. Today* **47**, 24 (1994).
3. J. M. Brase *et al.*, *Proc. Soc. Photo-Opt. Instrum. Eng.* **2201**, 474 (1994); S. S. Olivier *et al.*, *ibid.*, p. 1110.
4. R. Q. Fugate *et al.*, *Nature* **353**, 144 (1991).
5. D. Fried, *J. Opt. Soc. Am. A* **11**, 277 (1994); _____ and J. F. Belsher, *ibid.*, p. 227.
6. W. Happer, G. MacDonald, C. E. Max, F. Dyson, *ibid.*, p. 263.
7. R. Foy and A. Labeyrie, *Astron. Astrophys.* **152**, L29 (1985).
8. K. Avicola *et al.*, *J. Opt. Soc. Am. A* **11**, 825 (1994).
9. R. A. Humphreys, C. A. Primmerman, L. C. Bradley, J. Herrmann, *Opt. Lett.* **16**, 1367 (1991). Measurements of laser guide star centroid motion were made in two contiguous subapertures.
10. M. Lloyd-Hart *et al.*, *Astrophys. J.* **439**, 455 (1995). This system allowed control of relative tip-tilt between two (and, subsequently, all six) of the Multiple Mirror Telescope's 1.8-m primary mirrors.
11. S. S. Olivier *et al.*, *Proc. Soc. Photo-Opt. Instrum. Eng.* **2534**, 26 (1995).
12. A Shack-Hartmann sensor divides the telescope pupil into subapertures with the use of a set of miniature lenses (lenslet array) placed in a reimaged pupil plane. The average wave front slope in each subaperture was determined by measuring the position of the focused image formed by each lenslet. The constraint of continuity could then be imposed, and an estimate of the wave front phase could be reconstructed, for example, from a leastsquares fit.
13. Because the laser travels up through the turbulent atmosphere before forming the guide star, the instantaneous physical position of the guide star is variable. This upgoing beam wander results in a difference between the apparent instantaneous positions of a laser guide star and a natural star, rendering the laser guide star unsuitable as a reference for stabilization of the overall image position of astronomical objects. The solution is to use a faint natural star as overall tip-tilt reference. If this technique is used, the sky coverage for a laser guide star adaptive optics system is limited by the availability of suitable tip-tilt reference stars [S. S. Olivier, C. E. Max, D. Gavel, J. Brase, *Astrophys. J.* **407**, 428 (1993); (*14*)]. Because the requirements for a tip-tilt reference star are less severe than those for a high-order wave front reference beacon, the use of a laser guide star increases the sky coverage fraction for adaptive optics systems.
14. S. S. Olivier and D. T. Gavel, *J. Opt. Soc. Am. A* **11**, 368 (1994).
15. H. Friedman *et al.*, *Proc. Soc. Photo-Opt. Instrum. Eng.* **2201**, 352 (1994); H. W. Friedman *et al.*, *ibid.* **2534**, 150 (1995).
16. H. W. Friedman *et al.*, in *Proceedings of the European Southern Observatory, Conference No. 54* (European Southern Observatory, Garching, Germany, 1995), p. 207–211.
17. For the measured seeing conditions (0.8 arc sec at $\lambda = 2.2$ μm and $r_0 = 10.7$ cm at $\lambda = 0.55$ μm), direct integration of the modulation transfer function for telescope and ensemble-averaged atmosphere [D. L. Fried, *J. Opt. Soc. Am.* **56**, 1372 (1966); D. T. Gavel and S. S. Olivier, *Proc. Soc. Photo-Opt. Instrum. Eng.* **2201**, 295 (1994)] showed that the expected increase in peak intensity for tip-tilt correction was a factor of 3.7. However, taking into account the measured and inferred calibration errors of 1.7 rad^2 (assuming that they have roughly the same spectrum as the tilt-corrected atmosphere), the expected intensity increase was only a factor of 1.7. The measured value was 1.4. The degraded tip-tilt performance was attributable to misalignment of the tip-tilt sensor and nonoptimal tuning of the tip-tilt control parameters.
18. For a review, see J. M. Beckers, *Annu. Rev. Astron. Astrophys.* **31**, 13 (1993).
19. D. L. Fried, *J. Opt. Soc. Am.* **55**, 1427 (1965).
20. The factor by which the rms noise was reduced because of averaging by the control loop was estimated to be $\chi = [(2/\kappa) \tan^{-1} (\kappa/2)]^{1/2}$, where κ is the ratio of the sampling frequency to the control bandwidth (*13*).
21. Apart from the impact of finite laser spot size on measurement error (negligible in our experiments because of the very high signal to noise ratio), anisoplanatism due to finite laser spot size [R. Sasiela, *Technical Report No. 807* (Lincoln Laboratory, Lexington, MA, 1988)] contributed a mean square error of $\sigma^2 = (0.10146_{gs}/\theta_0)^{5/3} < 0.01$ for the parameters of our experiment, where $\theta_{gs} \sim 2$ arc sec is the laser spot size in the mesosphere and $\theta_0 = 3$ to 5 arc sec is the isoplanatic angle. Hence, finite laser spot size was not a significant factor in our data.

22. This work was performed under the auspices of the U.S. Department of Energy by the LLNL under contract number W 7405-Eng-48.

28 April 1997; accepted 5 August 1997

Requirement for GD3 Ganglioside in CD95- and Ceramide-Induced Apoptosis

Ruggero De Maria, Luisa Lenti, Florence Malisan, Federica d'Agostino, Barbara Tomassini, Ann Zeuner, Maria Rita Rippo, Roberto Testi*

Gangliosides participate in development and tissue differentiation. Cross-linking of the apoptosis-inducing CD95 protein (also called Fas or APO-1) in lymphoid and myeloid tumor cells triggered GD3 ganglioside synthesis and transient accumulation. CD95-induced GD3 accumulation depended on integral receptor "death domains" and on activation of a family of cysteine proteases called caspases. Cell-permeating ceramides, which are potent inducers of apoptosis, also triggered GD3 synthesis. GD3 disrupted mitochondrial transmembrane potential ($\Delta\Psi_m$), and induced apoptosis, in a caspase-independent fashion. Transient overexpression of the GD3 synthase gene directly triggered apoptosis. Pharmacological inhibition of GD3 synthesis and exposure to GD3 synthase antisense oligodeoxynucleotides prevented CD95-induced apoptosis. Thus, GD3 ganglioside mediates the propagation of CD95-generated apoptotic signals in hematopoietic cells.

CD95 is a surface receptor that triggers apoptotic cell death when cross-linked by its specific ligand (*1*). This is mediated by the recruitment of different cytosolic proteins to the "death domain" of the receptor, an ~70–amino acid protein-protein interaction domain that is essential for the generation of apoptotic signals. Seconds after the ligand induces the oligomerization of the receptor, the adaptor molecule FADD/MORT1 binds directly to the CD95 death domain, which in turn recruits caspase-8 (FLICE/MACH) (*2*). Other caspases then get activated in a proteolytic cascade, eventually leading to the hydrolysis of cytosolic and nuclear substrates (*3*).

Another pathway that depends on the death domain involves lipids and is also activated within 5 to 15 min after CD95 cross-linking (*4*): phosphatidylcholine-specific phospholipase C and acidic sphingomyelinase (ASM) are sequentially activated (*5*). Ceramides, generated from the hydrolysis of sphingomyelin by ASM, act as mediators of apoptosis in hematopoietic cells (*6*). Cells from individuals affected by Niemann-Pick disease, who are genetically deficient in ASM activity, or from mice in which the gene coding for ASM has been targeted, have defective apoptotic programs in response to radiation (*7*). However, the relevant targets of ceramides, or their metabolites, involved in downstream propagation of apoptotic signals remain poorly characterized. Newly synthesized or released ceramides are targeted to the Golgi complex and regulate sphingolipid and glycosphingolipid metabolism, including the rate of ganglioside biosynthesis within the Golgi (*8*). We therefore investigated whether changes in ganglioside metabolism could be detected during CD95 signaling.

Thin-layer chromatography (TLC) analysis of total cellular gangliosides revealed that when CD95 was cross-linked on HuT78, a cell line derived from a human

R. De Maria, F. Malisan, B. Tomassini, A. Zeuner, M. R. Rippo, R. Testi, Department of Experimental Medicine and Biochemical Sciences, University of Rome "Tor Vergata," 00133 Rome, Italy.

L. Lenti and F. d'Agostino, Department of Experimental Medicine and Pathology, University of Rome "La Sapienza," 00161 Rome, Italy.

*To whom correspondence should be addressed. E-mail: tesrob@flashnet.it

cutaneous T cell lymphoma, GD3 ganglioside was transiently accumulated, peaking in 15 min (Fig. 1A). Similar results were obtained by cross-linking CD95 on the human myeloid leukemia cell line U937, which also undergoes apoptosis upon CD95 stimulation (Fig. 1B). Clones of U937 and HuT78 that expressed CD95 receptors with defective death domains were resistant to apoptosis (*5*, *9*) and did not induce GD3 accumulation after CD95 cross-linking (Fig. 1B). Addition of the synthetic ceramide analogs C8-ceramide and C2-ceramide, both of which are cell-permeating and can directly induce apoptosis in HuT78 cells, resulted in GD3 accumulation that was maximal after 5 min. In contrast, the structurally related ceramide analog C2-dihydroceramide, which does not induce apoptosis, failed to induce GD3 (Fig. 1C). Accumulation of GD3 in HuT78 cells was confirmed by immunostaining of TLC plates with antibodies to GD3 (Fig. 1D). Quantitative analysis estimated a 5- to 10-fold increase in total cellular GD3 (up to 100 to 200 ng per 10^6 cells) in HuT78 cells after CD95 cross-linking or ceramide exposure (*10*). To investigate whether CD95-induced GD3 was derived by accelerated neosynthesis from GM3, HuT78 cells were loaded with pyrene-labeled GM3 and stimulated through CD95. After 15 min, fluorescent GD3 was clearly detectable by TLC analysis, which indicated that GD3 synthesis had been induced in vivo. Similarly, 5-min treatment of HuT78 cells with C8-ceramide could induce conversion of GM3 to GD3 in vivo (Fig. 1E). Thus, a GD3 synthase was responsible for both CD95- and ceramide-induced GD3 accumulation in intact cells (*11*) (Fig. 1F).

We subsequently investigated whether GD3 was directly involved in apoptosis. GD3 ganglioside, but not GD1a, GT1b, or GM1 gangliosides, induced apoptosis in HuT78 cells in a dose- and time-dependent manner as detected by ethidium bromide–acridine orange staining and fluorescence microscopy (Fig. 2, A and B), by flow cytometric analysis of hypodiploid nuclei (Fig. 2, C and D), and by internucleosomal DNA fragmentation agarose gel analysis (Fig. 2, E and F) in both lymphoid HuT78 cells and myeloid U937 cells (*12*).

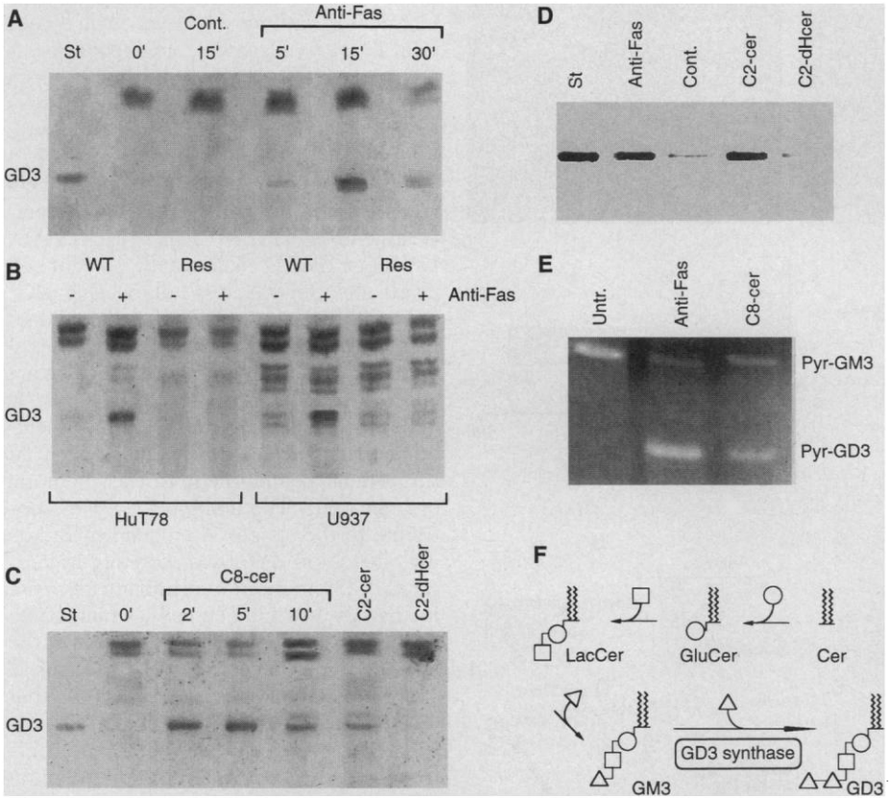

Fig. 1. GD3 synthesis follows CD95 cross-linking. (**A**) 30×10^6 mycoplasma-free HuT78 cells were treated with anti-Fas IgM (300 ng/ml; anti-CD95, CH-11; UBI, New York) or control IgM for the indicated times. st, standard; cont., control. (**B**) Wild-type (WT) HuT78 cells and U937 cells, as well as death domain–defective HuT78 (*5, 9*) and U937 CD95-resistant variants (res), were treated for 15 min with anti-Fas mAb (300 ng/ml) or left untreated. (**C**) 30×10^6 HuT78 cells were treated with 50 μM C8-ceramide for the indicated times or with 50 μM C2-ceramide (C2-cer) and 50 μM C2-dihydroceramide (C2-dHcer) for 5 min. All ceramides were from Biomol (Plymouth Meeting, PA). Cell extracts were run on HPTLC plates along with a GD3 authentic standard (st) and were visualized by resorcinol staining. (**D**) 2×10^6 HuT78 cells were treated with anti-Fas (300 ng/ml) or control mAb for 15 min and with 50 μM C2-ceramide or 50 μM C2-dihydroceramide for 5 min. Cell extracts were run on HPTLC plates along with a GD3 standard (st), and GD3 was detected by anti-GD3 immunostaining. (**E**) CD95 cross-linking and ceramide induce in vivo GD3 synthesis. 5×10^6 HuT78 cells loaded with pyrene-labeled (pyr-) GM3 were left untreated or were stimulated for 15 min with anti-Fas (300 ng/ml) or for 5 min with 50 μM C8-ceramide. Gangliosides were extracted, run on HPTLC plates, and visualized under a UV lamp (254 nm). (**F**) Steps to GD3 biosynthesis. Cer, ceramide; Glu Cer, glucosylceramide; Lac Cer, lactosylceramide; GM3, GM3 ganglioside; GD3, GD3 ganglioside. Circles, glucose; squares, galactose; triangles, sialic acid.

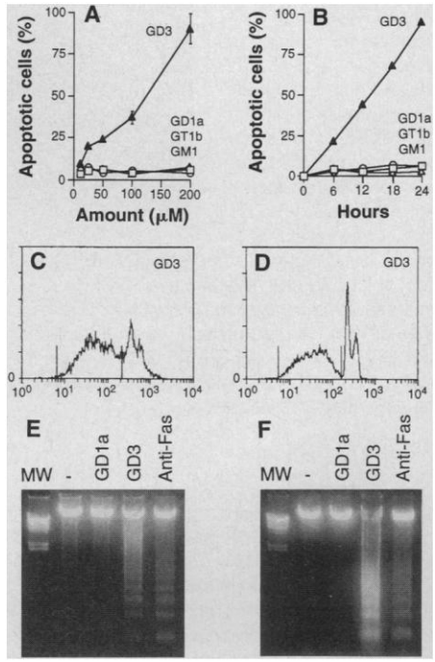

Fig. 2. GD3 induces apoptosis. (**A**) HuT78 cells were treated with different amounts of GD3 (solid triangles), GD1a, GT1b, and GM1 (open symbols), and cell viability was evaluated 24 hours later. GD3, GD1a, GT1b, and GM1 gangliosides were from Sigma. (**B**) HuT78 cells were treated with 200 μM GD3 (solid triangles) or 200 μM GD1a, GT1b, and GM1 (open symbols), and cell viability was evaluated at different time points. (**C**) HuT78 and (**D**) U937 cells were treated with 200 μM GD3, and DNA content in nuclei was assessed 12 hours later by propidium iodide staining and FACS analysis. Hypodiploid nuclei (included between vertical markers) were 55% in HuT78 cells and 48% in U937 cells. Hypodiploid nuclei were less than 5% in HuT78 or U937 cells treated with GD1a (not shown). (**E**) HuT78 cells and (**F**) U937 cells were left untreated or were treated with 200 μM GD1a, 200 μM GD3, or anti-Fas (100 ng/ml), and internucleosomal DNA fragmentation was assessed 12 hours later by DNA electrophoresis. MW, DNA molecular weight.

To verify that endogenous GD3 accumulation was also sufficient to trigger cell death, we transiently overexpressed in HuT78 cells the gene coding for GD3 synthase (α2,8-sialyltransferase), a transmembrane type II protein of about 40 kD that is resident in the early Golgi (*13*) and is responsible for GD3 synthesis by adding a second sialic acid to GM3. A GD3 synthase–green fluorescence protein fusion product (GFP-GD3 synthase) was expressed to identify transfected cells by fluorescence microscopy (Fig. 3, A through D). More than 90% of HuT78 cells that expressed GFP-GD3 synthase were dying within 24 hours (*14*). To exclude the possibility that protein overexpression in the Golgi was responsible for apoptosis, we expressed a GFP-GD3 synthase truncation mutant (GFP-ΔBH-GD3 synthase) that lacked most of the catalytic domain, including the COOH-terminal "sialyl motif S" [a highly conserved region among sialyltransferases (*13*)], but is still localized in the Golgi. The overexpression of the GFP-ΔBH-GD3 synthase mutant did not affect cell viability (Fig. 3E).

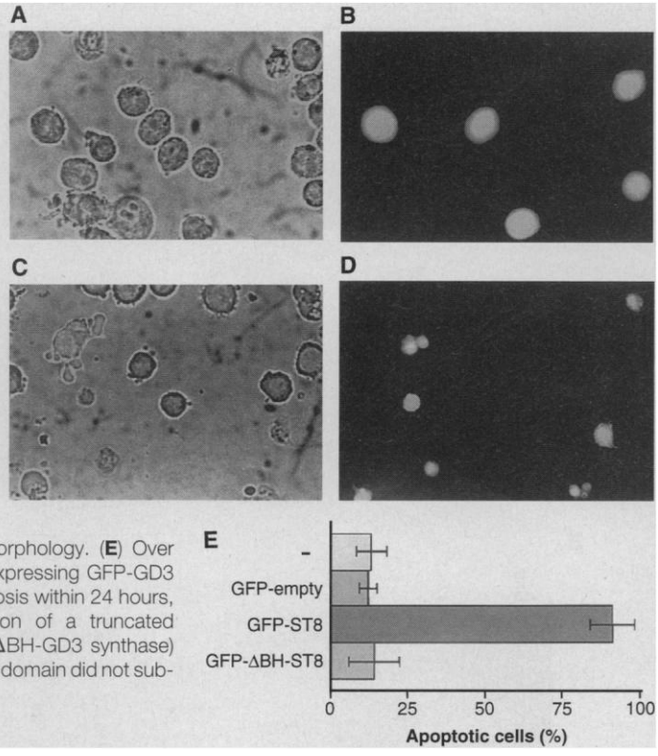

Fig. 3. GD3 synthase overexpression induces apoptosis. HuT78 cells were transfected with the pEGFP expression vector (**A**) and (**B**) or with a pEGFP-GD3 synthase expression vector (**C**) and (**D**). Cells were simultaneously evaluated by light microscopy to detect apoptotic cells [(A) and (C)] and by fluorescence microscopy to detect transfected cells [(B) and (D)]. Essentially all cells transfected with the pEGFP expression vector were alive, whereas most cells transfected with the pEGFP-GD3 synthase expression vector displayed apoptotic morphology. (**E**) Over 90% of HuT78 cells overexpressing GFP-GD3 synthase underwent apoptosis within 24 hours, whereas the overexpression of a truncated GFP-GD3 synthase (GFP-ΔBH-GD3 synthase) lacking most of the catalytic domain did not substantially affect cell viability.

We then asked whether GD3 accumulation after CD95 cross-linking and GD3-mediated apoptosis were caspase-dependent events. Pretreatment of HuT78 cells with caspase inhibitors YVAD and DEVD tetrapeptides prevented CD95-induced GD3 accumulation (Fig. 4A), which suggests that one or more proteolytic events were controlling accelerated GD3 synthesis after CD95 cross-linking. However, cell lysates from HuT78 cells undergoing apoptosis after direct GD3 exposure did not produce the in vitro cleavage of poly(ADP-rybose) polymerase (PARP), a common caspase substrate, unlike cell lysates from HuT78 cells undergoing apoptosis after CD95 cross-linking (Fig. 4B). Accordingly, pretreatment of HuT78 cells with YVAD, DEVD, or ZVAD could totally prevent cell death after CD95 cross-linking (Fig. 4C) but had little effect on GD3-mediated apoptosis (Fig. 4D), which suggests that relevant caspases were not direct downstream effectors of GD3 (*15*).

Disruption of the mitochondrial membrane potential ($\Delta\Psi_m$) is a crucial event in the cellular commitment to the apoptotic program (*16*). The ability of GD3 to contribute to the apoptotic program by inducing changes in $\Delta\Psi_m$ was therefore investigated. GD3 induced a significant decrease in the $\Delta\Psi_m$ of HuT78 cells, which could not be prevented by ZVAD, unlike the CD95-induced decrease in $\Delta\Psi_m$ (Fig. 4, E and F). Together, these data suggest that GD3-mediated signals autonomously contribute to the apoptotic program, probably through damage of mitochondrial function (*17*).

Finally, we investigated whether, by blocking GD3 synthesis, CD95-generated apoptotic signals could be interrupted. To interfere with ganglioside neosynthesis, we first used D-threo-1-phenyl-2-decanoylamino-3-morpholino-1-propanol (PDMP) as a potent cell permeating inhibitor of glucosyltransferase (*18*). Pretreatment of HuT78 cells with PDMP prevented GD3 accumulation after CD95 cross-linking (Fig. 5A) and was able to substantially block CD95-mediated apoptosis of HuT78 cells, but could not block GD3-mediated apoptosis (Fig. 5B). Second, we directly targeted GD3 synthase expression by antisense oli-

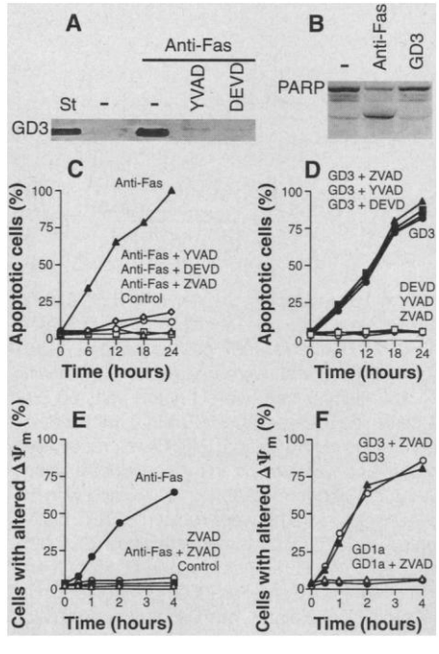

Fig. 4. Caspase activation controls GD3 accumulation. (**A**) 5×10^6 HuT78 cells were preincubated for 30 min with 200 μM Ac-DEVD-CHO and 400 μM Ac-YVAD-CMK, then stimulated with anti-Fas (300 ng/ml). GD3 accumulation was evaluated after 15 min by immunostaining with R24 mAb. (**B**) HuT78 cells were treated with anti-Fas (300 ng/ml) or 200 μM GD3 for 3 hours; then 15 μl of control, anti-Fas, or GD3-stimulated HuT78 cell lysates was incubated with in vitro–translated [^{35}S]PARP. (**C**) HuT78 cells were preincubated for 30 min with 200 μM Ac-DEVD-CHO, 400 μM Ac-YVAD-CMK, or 40 μM ZVAD-FMK, then stimulated with anti-Fas (100 ng/ml). The percentage of apoptotic cells was assessed at the indicated times by ethidium bromide–acridine orange staining and fluorescence microscopy. (**D**) HuT78 cells were pre-incubated for 30 min with 200 μM Ac-DEVD-CHO, with 400 μM Ac-YVAD-CMK, or 40 μM ZVAD-FMK, then stimulated with 200 μM GD3. The percentage of apoptotic cells was assessed at the indicated times by ethidium bromide–acridine orange staining and fluorescence microscopy. (**E** and **F**) HuT78 cells were left untreated or pre-incubated for 30 min with 40 μM ZVAD-FMK, then stimulated with anti-Fas (200 ng/ml), 200 μM GD1a, or 200 μM GD3, and the percentage of cells with disrupted $\Delta\Psi_m$ was evaluated by staining with 5,5′,6,6′-tetrachloro-1,1′,3,3′-tetraethylbenzimidazolcarbocyanine iodide (JC-1) and flow cytometry.

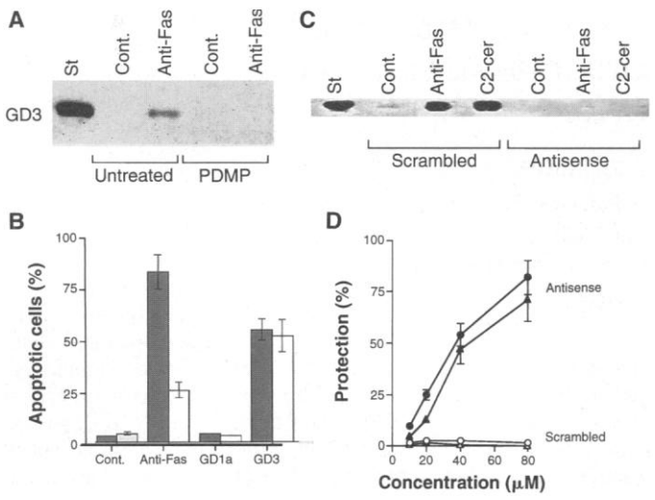

Fig. 5. Preventing GD3 synthesis blocks CD95 apoptotic signals. (**A**) HuT78 cells were incubated for 36 hours with 20 μM PDMP or left untreated, then stimulated for 15 min with anti-Fas (300 ng/ml) or control IgM. GD3 was visualized by resorcinol staining. (**B**) HuT78 cells were incubated for 36 hours with 20 μM PDMP (gray bars) or left untreated (white bars), then stimulated for 12 hours with control IgM, anti-Fas (100 ng/ml), 200 μM GD1a, or 200 μM GD3. Cell viability was assessed by ethidium bromide–acridine orange staining and fluorescence microscopy. Means ± 1 SD from four different experiments are shown. (**C**) HuT78 cells were incubated for 48 hours with 80 μM of GD3 synthase antisense oligodeoxynucleotide or with a scrambled sequence from the same deoxynucleotides, then treated with control IgM, anti-Fas (300 ng/ml), or 50 μM C8-ceramide. GD3 accumulation was evaluated after 15 min by immunostaining with R24 antibody. (**D**) HuT78 cells were incubated for 72 hours with the indicated concentrations of GD3 synthase antisense (solid symbols) or scrambled (open symbols) oligodeoxynucleotides, then treated with anti-Fas (100 ng/ml) (circles) or 50 μM C2-ceramide (triangles). Apoptosis was assessed 12 hours later by propidium iodide staining of nuclei and FACS analysis. Means ± 1 SD from five different experiments are shown.

godeoxynucleotides. Exposure to GD3 synthase antisense oligodeoxynucleotides encompassing the 5′ region of the gene surrounding the second initiator ATG (*19*), but not to a scrambled sequence of the same oligodeoxynucleotides, suppressed both basal and CD95-induced or C8-ceramide–induced GD3 synthesis (Fig. 5C), which indicates that GD3 was generated by neosynthesis rather than by degradation from more complex gangliosides. Exposure to GD3 synthase antisense prevented both CD95-mediated and C8-ceramide–mediated apoptosis effectively and in a dose-dependent manner (Fig. 5D) (*20*).

The data presented here provide the first evidence for an involvement of gangliosides, specifically GD3 ganglioside, in programmed cell death. GD3 might mediate apoptotic signals that follow intracellular ceramide accumulation through recruitment of mitochondria to the apoptotic program. Newly synthesized gangliosides can be shuttled from the Golgi to mitochondria (*21*), and gangliosides are known to affect the ion permeability of biological membranes (*22*). In the CD95 system, CD95-induced GD3 synthesis and transient accumulation require intact receptor death domains and upstream caspase activation. Rapidly accumulated GD3 can then alter mitochondrial function and promote cell death in a caspase-independent manner. Because direct interference with endogenous GD3 synthesis by targeting of GD3 synthase prevented CD95-induced apoptosis, our data also point towards the early Golgi, where GD3 synthase is localized, as a critical subcellular compartment for the progression of apoptotic signals.

REFERENCES AND NOTES

1. S. Nagata and P. Golstein, *Science* **267**, 1449 (1995); P. H. Krammer *et al.*, *Immunol. Rev.* **142**, 175 (1994).
2. M. Muzio *et al.*, *Cell* **85**, 817 (1996); M. P. Boldin, T. M. Goncharov, Y. V. Goltsev, D. Wallach, *ibid.*, p. 803.
3. M. Los *et al.*, *Nature* **375**, 81 (1995); M. Enari, H. Hug, S. Nagata, *ibid.*, p. 78.
4. R. Testi, *Trends Biochem. Sci.* **21**, 468 (1996).
5. M. G. Cifone *et al.*, *J. Exp. Med.* **180**, 1547 (1994); M. G. Cifone *et al.*, *EMBO J.* **14**, 5859 (1995); R. De Maria *et al.*, *J. Clin. Invest.* **97**, 316 (1996).
6. Y. A. Hannun and L. M. Obeid, *Trends Biochem. Sci.* **20**, 73 (1995); L. M. Obeid, C. M. Linardic, L. A. Karolak, Y. A. Hannun, *Science* **259**, 1769 (1993); S. Mathias and R. Kolesnick, *Adv. Lipid Res.* **25**, 65 (1993); R. Kolesnick and Z. Fuks, *J. Exp. Med.* **181**, 1949 (1995).
7. P. Santana *et al.*, *Cell* **86**, 189 (1996).
8. D. Allan and K.-J. Kallen, *Progr. Lipid Res.* **32**, 195 (1993); G. van Echten and K. Sandhoff, *J. Biol. Chem.* **268**, 5341 (1993).
9. I. Cascino, G. Papoff, R. De Maria, R. Testi, G. Ruberti, *J. Immunol.* **156**, 13 (1996).
10. R. De Maria *et al.*, unpublished results.
11. Cells were disrupted by two cycles of freezing and thawing. Polar lipids were then extracted, and gangliosides were chromatographed on silica gel 60 high-performance thin-layer chromatography (HPTLC) plates (Merck; Darmstadt, Germany), dried, and visualized with resorcinol. For immunostaining, plates were treated with 0.5% polyisobutylmetacrylate in hexane, dried, incubated for 1 hour with R24 monoclonal antibody (mAb) to GD3 (IgG_3), and revealed by immunoperoxidase staining. For fluorescent ganglioside studies, cells were incubated for 30 min at 37°C with pyrene-labeled GM3, then stimulated. Gangliosides were then extracted and chromatographed on HPTLC plates. Pyrene-conjugated gangliosides were visualized with an ultraviolet (UV) lamp at 254 nm.
12. Cell viability was evaluated by ethidium bromide–acridine orange staining and fluorescence microscopy. Hypodiploid nuclei were evaluated by hypotonic propidium iodide solution staining and flow cytometric analysis, with the use of a FACScan (Becton Dickinson; San Jose, CA). Internucleosomal DNA fragmentation was analyzed by DNA electrophoresis.
13. K. Sasaki *et al.*, *J. Biol. Chem.* **269**, 15950 (1994); K. Nara *et al.*, *Proc. Natl. Acad. Sci. U.S.A.* **91**, 7952 (1994); M. Haraguchi *et al.*, *ibid.*, p. 10455.
14. The GD3 synthase cDNA was cloned in the PUC vector, and a 1152–base pair (bp) Apa I fragment was further cloned in the pEGFP-C3 expression vector (Clontek; Palo Alto, CA). The ΔBH deletion mutant was generated by removing the COOH-terminal portion of the enzyme with Bam HI. The 514-bp Bam HI–Apa I fragment was then cloned in pEGFP-C3. HuT78 cells were electroporated (Gene Pulser, Bio-Rad; Hercules, CA), and viable cells were recovered by lymphoprep density gradient centrifugation. After 24 hours of culture, cells were analyzed by fluorescence microscopy. Transfection efficiency was typically 20 to 25% as measured by fluorescence emission.
15. Coupled transcription and translation of PARP, cloned into the pGEM plasmid under the T7 promoter, was performed with the TNT kit (Promega, Madison, WI). Each reaction was carried out for 2 hours at 37°C, then samples were resolved by 10% SDS–polyacrylamide gel electrophoresis and autoradiographed. Caspase inhibitors Ac-YVAD-CMK (Ac–Tyr-Val-Ala-Asp–chloromethylketone), Ac-DEVD-CHO (Ac–Asp-Glu-Val-Asp–CHO), and ZVAD-FMK (*N*-benzyloxycarbonyl–Val-Ala-Asp–fluoromethylketone) were from Bachem (Bubendorf, Switzerland).
16. G. Kroemer, N. Zamzami, S. A. Susin, *Immunol. Today* **18**, 44 (1997).
17. B. S. Polla *et al.*, *Proc. Natl. Acad. Sci. U.S.A.* **93**, 6458 (1996). After stimulation, 5×10^5 cells per milliliter were incubated for 15 min with JC-1 (10 μg/ml) (Molecular Probes; Eugene, OR). Cells were then washed twice with cold phosphate-buffered saline and immediately analyzed by flow cytometry. JC-1 forms red fluorescent J aggregates (590 nm) at higher $\Delta\Psi_m$ and green fluorescent monomers (527 nm) at low membrane potentials. Changes in $\Delta\Psi_m$ were therefore evaluated by the shift in fluorescence emission.
18. N. S. Radin, J. A. Shayman, J.-I. Inokuchi, *Adv. Lipid Res.* **26**, 183 (1993); N. S. Radin and R. R. Vunnan, *Methods Enzymol.* **72**, 673 (1981).
19. G. Zeng, T. Ariga, X.-b. Gu, R. K. Yu, *Proc. Natl. Acad. Sci. U.S.A.* **92**, 8670 (1995).
20. PDMP was from Matreya (Pleasant Gap, PA). The GD3 synthase antisense oligodeoxynucleotide sequence (5′-CAGTACAGCCATGGCCCCTCT-3′) was selected on the 5′ region of the gene surrounding the second initiator ATG. A scrambled sequence from the same deoxynucleotides (5′-CGACCTAC-CTATGCGCTACCG-3′) was also used as a control. To increase nuclease resistence, both oligodeoxynucleotide sequences were phosphorothioate-modified on every second deoxynucleotide.
21. G. R. Matyas and D. J. Morré, *Biochim. Biophys. Acta*, **921**, 599 (1987).
22. P. Sarti *et al.*, *Biochem. J.* **267**, 413 (1990); G. Tettamanti and L. Riboni, *Prog. Brain Res.* **101**, 77 (1994).

23. We thank T. Nishi (Tokyo Research Laboratories, Japan); L. J. Old (Ludwig Institute, New York); R. Beyaert (University of Ghent, Belgium) for kindly providing reagents; and V. Zacchei for expert assistance. Supported by grants to R.T. from Associazione Italiana Ricerca sul Cancro (AIRC), Consiglio Nazionale delle Ricerche (CNR), Ministero dell'Universitá e della Ricerca Scientifica e Tecnologica (MURST), and the European Community Biomed 2 and Human Capital and Mobility Programs. R.D.M. is an AIRC fellowship holder.

18 March 1997; accepted 15 July 1997